Gastrointestinal stromal tumors in the duodenum show increased contrast enhancement compared with those in the stomach on computed tomography

RYOSUKE SATO[1,2], RYO HARADA[1], KENJI HASHIMOTO[1], TOMOAKI TSUTSUI[1], NAO HATTORI[1], MASAFUMI INOUE[1], HARUHIKO KOBASHI[1], MAMI MORIMOTO[3], MAIKO TAMURA[3], ATSUSHI HAYASHI[4] and MASAYA IWAMURO[2]

[1]Department of Gastroenterology and Hepatology, Japanese Red Cross Okayama Hospital, Okayama 700-8607; [2]Department of Gastroenterology and Hepatology, Okayama University Hospital, Okayama 700-8558; Departments of [3]Radiology and [4]Pathology, Japanese Red Cross Okayama Hospital, Okayama 700-8607, Japan

Received May 16, 2022; Accepted July 25, 2022

DOI: 10.3892/mco.2022.2577

Abstract. Duodenal gastrointestinal stromal tumors (D-GISTs) are a rare and relatively small subset of GISTs whose imaging features are not well known. The present study aimed to evaluate the enhancement pattern of D-GISTs compared with that of gastric GISTs (G-GISTs) using dynamic computed tomography. This single-center, retrospective, clinicopathological analysis was conducted on 10 patients with D-GISTs who underwent surgery between June 2006 and October 2018. In the same period, 25 patients with G-GISTs underwent surgery and were enrolled. The contrast ratio was defined as the ratio between Hounsfield units in contrast enhanced and unenhanced images in different phases, and these ratios were compared between the D-GIST and G-GIST groups. Furthermore, microvessel density, analyzed by immunohistochemical staining for CD31, was compared between the D-GIST and G-GIST groups. The contrast ratio of D-GIST was significantly higher than that of G-GIST in the arterial, portal and delayed phases ($P<0.01$, $P<0.01$ and $P=0.02$, respectively). The microvessel density of the D-GISTs was significantly higher than that of the G-GISTs ($P<0.0001$). D-GISTs were more hypervascular than G-GISTs on both imaging and pathological analyses.

Correspondence to: Dr Ryosuke Sato, Department of Gastroenterology and Hepatology, Japanese Red Cross Okayama Hospital, 2-1-1 Aoe, Kita-ku, Okayama 700-8607, Japan
E-mail: rsato0731@gmail.com

Abbreviations: CT, computed tomography; GIST, gastrointestinal stromal tumor; D-GIST, duodenal GIST; G-GIST, gastric GIST; PSPDA, posterior superior pancreaticoduodenal artery; ROI, region of interest; SMA, superior mesenteric artery; VEGF, vascular endothelial growth factor

Key words: GIST, hypervascular, CT, anti-CD31 antibody, immunochemistry

Introduction

Gastrointestinal stromal tumors (GISTs), which originate from interstitial cells of Cajal, are the most common submucosal tumors of the gastrointestinal tract. GISTs can occur anywhere in the gastrointestinal tract, most commonly in the stomach (50-70%), followed by the jejunum and ileum (25-35%), and colon (5%); only 5% of GISTs are reported to occur in the duodenum (1,2). Liu *et al* (3) reported that the prognosis of patients with duodenal GISTs (D-GISTs) was significantly worse than that of patients with gastric GISTs (G-GISTs). Although studies involving D-GISTs have been published, most included a small number of samples owing to the infrequency of GISTs. In addition, few studies have investigated the computed tomography (CT) features of D-GISTs (4).

Therefore, we conducted this retrospective study to compare the CT findings between D-GISTs and G-GISTs. We also performed immunohistochemical staining for CD31 to confirm microvessel density in the D-GIST and G-GIST specimens.

Materials and methods

Patients. Between June 2006 and October 2018, 10 patients with D-GISTs and 27 patients with G-GISTs underwent surgery at the Japanese Red Cross Okayama Hospital. Two patients with G-GISTs who did not undergo dynamic CT before surgical resection were excluded. Therefore, a final 35 patients were retrospectively investigated. GIST was diagnosed based on the histopathological evaluation of the resected specimen. The degree of recurrence risk of D-GISTs and G-GISTs was determined according to the modified Fletcher classification (5). The study design was approved by the ethics committee of our institute and adhered to the principles of the Declaration of Helsinki. Informed consent was obtained from all patients.

CT protocol. Multidetector CT was used to perform triphasic spiral CT on 35 patients (Aquilion ONE; Canon Medical Systems) with the following scanning settings: 120 kVp, 360 mA, 2-mm section collimation, and an 11.0 mm/sec table

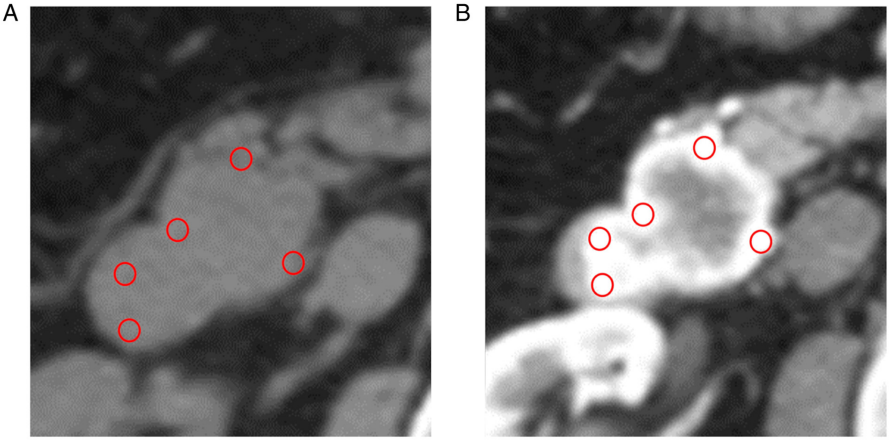

Figure 1. Contrast-enhanced CT images of a duodenal gastrointestinal stromal tumor in a patient. (A) Plain CT image. (B) CT image obtained in the arterial phase. Five regions of interest (red circles) were placed to measure CT values. CT, computed tomography.

speed. To capture adjacent parts, images were reconstructed every 5 mm. Non-ionic iodinated contrast material (2 ml/kg, iopamidol, Iopamiron 370; Bayer, Leverkusen, Germany) was administered into the vein using a power injector at a flow rate of 3.2 ml/sec. At 12, 32, and 180 sec after the contrast material was injected, arterial, portal, and delayed phase spiral scans were automatically commenced.

Quantitative evaluation of dynamic CT. Unenhanced and contrast-enhanced images were available for each patient during the arterial, portal, and delayed phases. To determine the tumor enhancement grade, CT attenuation values of the lesion were measured in Hounsfield units using circular regions of interest (ROIs). Five ROIs were placed on the most strongly enhanced portion of the lesion in each arterial, portal, and delayed phase. Each ROI was placed in approximately the same area, and we measured the CT attenuation values of unenhanced lesions in similar areas (Fig. 1). Five ROI values for each phase or for the unenhanced phase were averaged. The contrast ratio was determined by taking the ratio of the averaged ROI values of lesions in each phase and in the unenhanced phase.

Assessment of vascularity. Formalin-fixed and paraffin-embedded sections at 4-μm thickness were used for immunohistochemical staining of surgically resected tissue samples. Immunohistochemistry was carried out using conventional procedures. Anti-CD31 monoclonal antibodies (clone JC70A; Novocastra, England) were used to identify vascular endothelial cells, and hematoxylin was used to counterstain the sections. Tissue slices with CD31 staining were inspected under low magnification (x40) to select the three most vascularized regions inside the tumor. The microvessel densities in these regions were subsequently quantified as the ratios between the CD31-stained and -unstained areas within the selected tumor sections at high magnification (x100) using Adobe Photoshop Elements (version 14.0; Adobe Systems). The microvessel density value for the tumor sample was computed using the mean value of the microvessel densities of the three selected areas. The microvessel density values of D-GISTs and G-GISTs were compared.

Statistical analysis. JMP software version 12.2.0 was used to perform statistical calculations (SAS Institute, Inc.). Categorical values were compared with Fisher's exact test. Continuous values were compared using the Mann-Whitney U test or the Kruskal-Wallis test followed by Dunn's test. Correlation coefficients were analyzed using Pearson's correlation. $P<0.05$ was considered to indicate a statistically significant difference. No correction for multiple hypothesis testing was used because this was an exploratory study.

Results

Patient characteristics. The backgrounds of the study participants are shown in Table I. Between these two groups, no significant differences were observed regarding age, sex, presence or absence of symptoms, tumor size, presence or absence of calcification, or risk classification. With respect to location, D-GISTs were most frequently observed in the 2nd portion of the duodenum (7/10, 70.0%). G-GISTs were predominantly identified in the gastric corpus (18/25, 72.0%).

Contrast ratio in each phase. The contrast ratios of D-GISTs and G-GISTs in each phase are shown in Fig. 2. The contrast ratio of D-GISTs was significantly higher than that of G-GISTs in the arterial (6.52±2.77 vs. 2.41±0.98, $P<0.01$), portal (4.67±1.74 vs. 2.66±1.21, $P<0.01$), and delayed phases (3.64±1.43 vs. 2.81±1.16, $P=0.02$). The difference in contrast ratio between D-GISTs and G-GISTs was largest in the arterial phase.

Correlation between microvessel density and CT contrast ratio. Representative images of CD31 immunostaining in G-GISTs and D-GISTs are presented in Fig. 3A and B, respectively. CD31-positive microvessels scarcely existed in G-GISTs, whereas there were plenty of microvessels in D-GISTs. As shown in Fig. 4, D-GISTs had a higher microvessel density than G-GISTs (5.52±3.98 vs. 0.35±0.19, $P<0.0001$).

There was a significant correlation between microvessel density and the contrast ratio in D-GISTs (Fig. 5).

Comparison of contrast ratios between risk classifications. According to the modified Fletcher classification, D-GISTs

Table I. Baseline characteristics of the patients.

Variable	Duodenal GISTs (n=10)	Gastric GISTs (n=25)	P-value
Mean age, years (range)	60.90 (43.00-87.00)	68.80 (47.00-82.00)	0.35
Sex, n (male/female)	5/5	12/13	0.64
Symptom, n			
Abdominal pain	0	2	
Bleeding	3	2	
Fatigue	1	1	
Location	1/7/1/1 (1st/2nd/3rd/4th)	6/18/1 (fundus/body/antrum)	
Median tumor size, mm (range)	38.00 (10.00-71.00)	32.00 (14.00-160.00)	0.76
Calcification, n			0.74
Present	1	3	
Absent	9	22	
Degree of risk, n			0.23
Very low	2	3	
Low	6	12	
Intermediate	0	5	
High	2	5	

GIST, gastrointestinal stromal tumor.

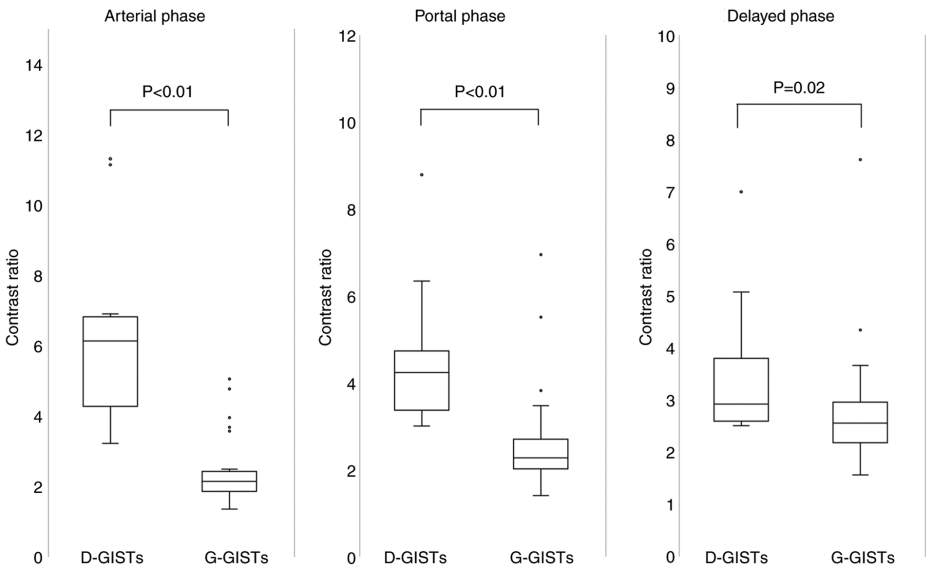

Figure 2. Contrast ratios of D-GISTs and G-GISTs in the arterial, portal and delayed phases. The contrast ratio in each phase differed significantly between the D-GIST and G-GIST groups. D-GIST, duodenal gastrointestinal stromal tumor; G-GIST, gastric gastrointestinal stromal tumor.

were classified as very low risk (n=2), low risk (n=6), or high risk (n=2). G-GISTs were classified as very low risk (n=3), low risk (n=12), intermediate risk (n=5), or high risk (n=5). Fig. 6 shows the correlation between the contrast ratio in the arterial phase and risk classification in D-GISTs and G-GISTs. The contrast ratio did not differ between the risk grades.

Discussion

In the present study, we showed that D-GISTs had a larger CD31-positive area than G-GISTs. This result was consistent with the fact that D-GISTs may appear as hypervascular lesions. The duodenum is divided into four portions; it has been reported that the feeding arteries of the first and second portions of the duodenum are different from those of the third and fourth portions (6). The first and second portions of the duodenum are nourished by the posterior superior pancreaticoduodenal artery (PSPDA), which branches from the gastroduodenal artery. The PSPDA and the inferior pancreaticoduodenal artery form an arcade called the pancreaticoduodenal arcade. The third and fourth portions are nourished by the first jejunal artery, which branches from the superior mesenteric artery

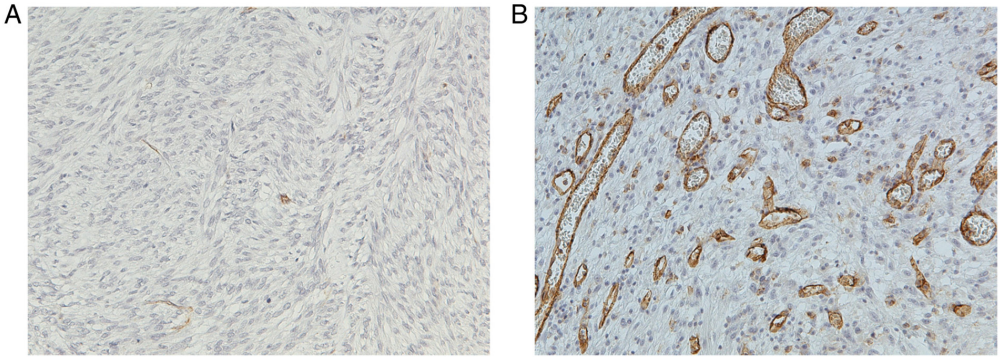

Figure 3. Immunohistochemical staining with anti-CD31 antibodies. (A) Gastric gastrointestinal stromal tumor (original magnification, x100). (B) Duodenal gastrointestinal stromal tumor. The brownish areas are positive for CD31 (original magnification, x100).

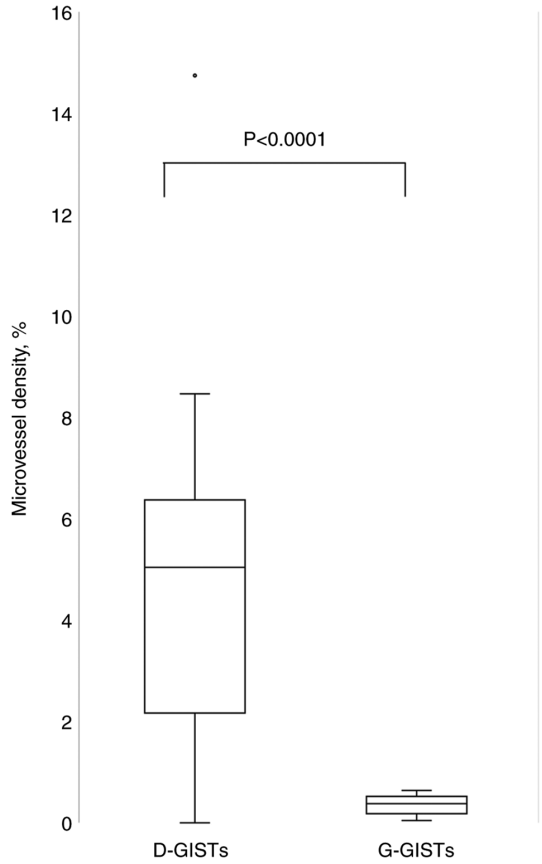

Figure 4. Comparison of microvessel density in D-GISTs and G-GISTs. There was a significant difference in microvessel density between the D-GIST and G-GIST groups. D-GIST, duodenal gastrointestinal stromal tumor; G-GIST, gastric gastrointestinal stromal tumor.

(SMA). The vasculature of G-GISTs has been reported in two cases (7). Cai *et al* (8) reported on the vasculature of D-GISTs, especially the importance of the supply arteries and drainage veins in differential diagnosis. According to their report, the vasculature of D-GISTs from each portion was consistent with that of the normal duodenum, and it was difficult to find the obvious supply arteries for duodenal adenocarcinoma or lymphoma. Furthermore, 50% of D-GISTs drain directly into the portal venous trunk, which is not detected in other duodenal tumors (8). Futo *et al* (9) reported that D-GISTs arising from the second or third portions of the duodenum may be incorrectly diagnosed as pancreatic neuroendocrine tumors. Thus, some studies have shown the features of D-GIST imaging findings; however, the reason why D-GISTs show hypervascularity remains unexplained. We hypothesized that one of the reasons why D-GISTs display hypervascularity is due to the large number and complexity of the duodenal feeding arteries.

Using immunohistochemical staining samples, we found that microvessel density in D-GISTs was greater than that in G-GISTs, and there was a significant correlation between the contrast ratio and microvessel density in D-GISTs. The correlation between dynamic CT findings and microvessel density has been reported in pancreatic ductal adenocarcinoma (10), pancreatic neuroendocrine neoplasm (11), and prostate disease (12). A correlation between microvessel density and clinical characteristics has been reported for GISTs. However, to the best of our knowledge, no previous study has investigated the correlation between microvessel density and dynamic CT findings. We believe that the degree of vascularity has a significant relationship with microvessel density in D-GISTs.

A previous report showed that high-grade GISTs had higher CT attenuation values than intermediate-, low-, or very low-grade GISTs in the arterial phase (13). However, we found no significant difference between the contrast ratio and degree of risk. We used the modified Fletcher classification system to evaluate the risk of recurrence. The modified Fletcher classification is defined by tumor size and mitotic index (4). We discovered a significant correlation between the contrast ratio and microvessel density in D-GISTs. Therefore, if there is a correlation between microvessel density and the mitotic index, there may also be a correlation between the contrast ratio and risk classification. Microvessel density has a strong positive correlation with the degree of malignancy of intraductal papillary mucinous neoplasms of the pancreas (14) and colorectal tumors (15). In the case of GISTs, high CD31 values, in other words, high microvessel density, were reported to be related to poor prognosis (16). Meanwhile, other researchers have reported that microvessel density was not significantly correlated with mitosis (17). The fact that 80% of the D-GISTs in this study were in the very low or low risk group despite their poor prognosis may be related to the fact that there was no significant correlation between contrast ratio and risk classification. At this stage, we cannot assert a correlation between the microvessel density and the mitotic index. Therefore,

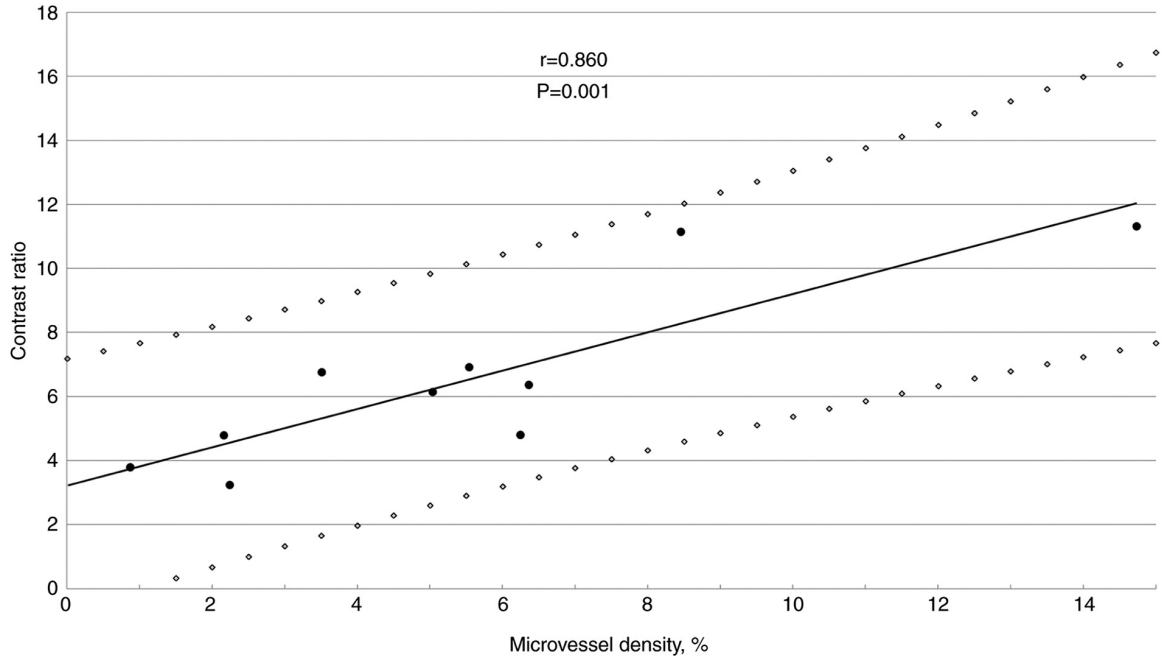

Figure 5. Correlation between the microvessel density and the contrast ratios in duodenal gastrointestinal stromal tumors. A strong, positive linear correlation between microvessel density and the contrast ratios (Pearson's correlation; r=0.860; P=0.001) was observed.

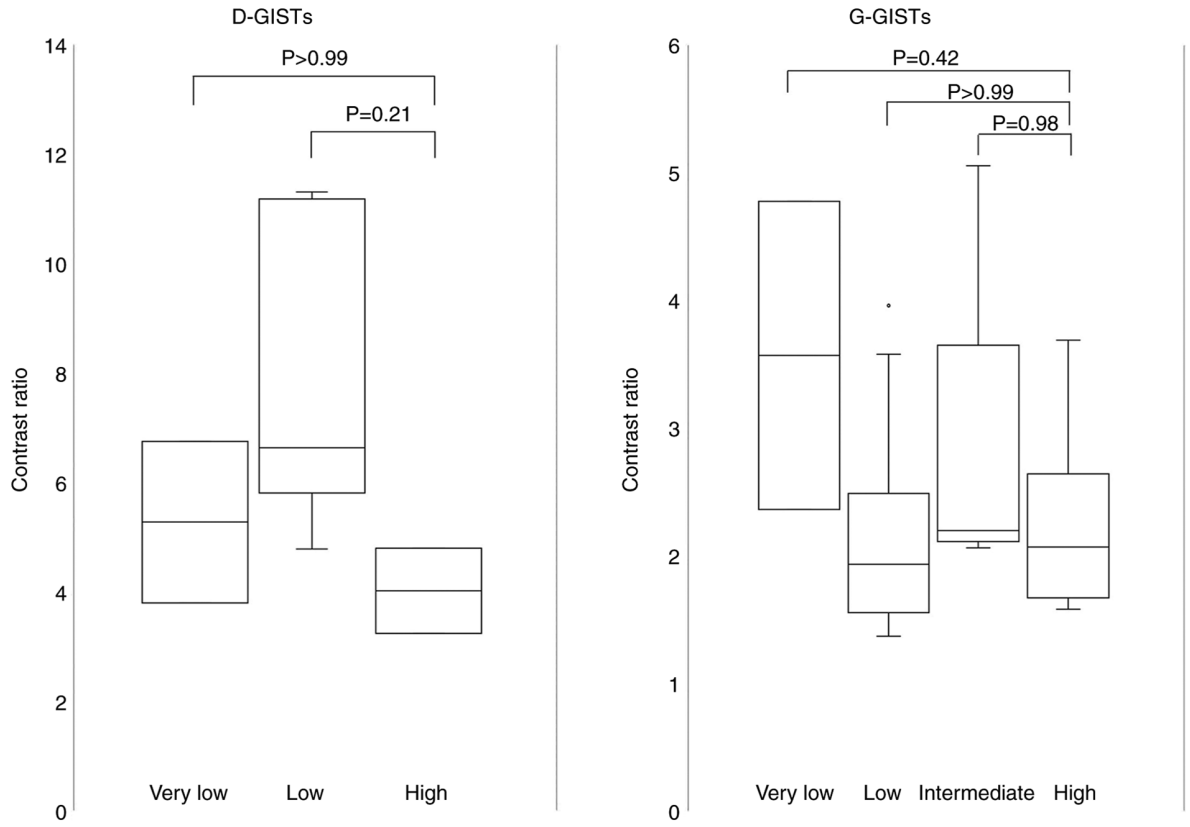

Figure 6. Comparison of the contrast ratios for each risk classification in D-GISTs and G-GISTs. No significant difference was observed among risk classifications. D-GIST, duodenal gastrointestinal stromal tumor; G-GIST, gastric gastrointestinal stromal tumor.

we investigated the correlation between mitosis as a risk classification factor and microvessel density.

Imamura *et al* (17) reported that there was significant correlation between microvessel density and vascular endothelial growth factor (VEGF) expression in GISTs. VEGF plays a major role in promoting tumor angiogenesis (18). The authors also found that intestinal GISTs had greater VEGF expression and microvessel density than G-GISTs (17). This may explain

why D-GISTs are more hypervascular than G-GISTs. Further research on VEGF, other angiogenic factors, and genetic abnormalities of GISTs may lead to treatments targeting them.

Our study had some limitations. First, this was a retrospective case study with a small cohort, and all dynamic CT scans were performed at a single institution. D-GISTs are relatively rare, and we could only analyze 10 D-GIST cases in our institution. Further investigation with more cases from multiple institutions is needed to reveal the imaging and pathological features of D-GISTs. Second, we attempted to perform microvessel analysis at the most vascularized region inside the tumor. However, the region of GISTs where we analyzed the microvessel density and CT ratio may be slightly different.

In summary, the results of our analyses demonstrated that D-GISTs were more hypervascular than G-GISTs on imaging and pathological examination. The reason why D-GISTs are more hypervascular than G-GISTs remains uncertain. However, we speculate that this involves two components: Anatomical and molecular biology. In other words, D-GISTs have large feeding arteries and drainage veins that are sufficient for detection and greater VEGF expression than G-GISTs.

Acknowledgements

Not applicable.

Funding

No funding was received.

Availability of data and materials

The datasets used and/or analyzed during the current study are available from the corresponding author on reasonable request.

Authors' contributions

RS wrote the manuscript and made substantial contributions to conception and design, and acquisition of data. RH and KH made substantial contributions to analysis and interpretation of data. TT, NH, MIn and HK assisted in the statistical procedures. MM made substantial contributions to the analysis and interpretation of data of CT imaging. MT, AH and MIw made substantial contributions to the analysis and interpretation of data of the pathological examinations. RS and RH confirmed the authenticity of all the raw data. All authors read and approved the final manuscript.

Ethics approval and consent to participate

The study design was approved by the ethics committee of Japanese Red Cross Okayama Hospital (Okayama, Japan) and adhered to the principles of the Declaration of Helsinki. Written informed consent was obtained from all patients.

Patient consent for publication

Written informed consent was obtained from the patients for publication of this study and any accompanying images.

Competing interests

The authors declare that they have no competing interests.

References

1. Joensuu H: Gastrointestinal stromal tumor (GIST). Ann Oncol 17: x280-x286, 2006.
2. Scola D, Bahoura L, Copelan A, Shirkhoda A and Sokhandon F: Getting the GIST: A pictorial review of the various patterns of presentation of gastrointestinal stromal tumors on imaging. Abdom Radiol (NY) 42: 1350-1364, 2017.
3. Liu Z, Zheng G, Liu J, Liu S, Xu G, Wang Q, Guo M, Lian X, Zhang H and Feng F: Clinicopathological features, surgical strategy and prognosis of duodenal gastrointestinal stromal tumors: A series of 300 patients. BMC Cancer 18: 563, 2018.
4. Sandrasegaran K, Rajesh A, Rushing DA, Rydberg J, Akisik FM and Henley JD: Gastrointestinal stromal tumors: CT and MRI findings. Eur Radiol 15: 1407-1414, 2005.
5. Joensuu H, Vehtari A, Riihimäki J, Nishida T, Steigen SE, Brabec P, Plank L, Nilsson B, Cirilli C, Braconi C, *et al*: Risk of recurrence of gastrointestinal stromal tumour after surgery: An analysis of pooled population-based cohorts. Lancet Oncol 13: 265-274, 2012.
6. Desai GS and Pande PM: Gastroduodenal artery: Single key for many locks. J Hepatobiliary Pancreat Sci 26: 281-291, 2019.
7. Teoh WC, Teo SY and Ong CL: Gastrointestinal stromal tumors presenting as gynecological masses: Usefulness of multidetector computed tomography. Ultrasound Obstet Gynecol 37: 107-109, 2011.
8. Cai PQ, Lv XF, Tian L, Luo ZP, Mitteer RA Jr, Fan Y and Wu YP: CT characterization of duodenal gastrointestinal stromal tumors. AJR Am J Roentgenol 204: 988-993, 2015.
9. Futo Y, Saito S, Miyato H, Sadatomo A, Kaneko Y, Kono Y, Matsubara D, Horie H, Lefor AK and Sata N: Duodenal gastrointestinal stromal tumors appear similar to pancreatic neuroendocrine tumors: A case report. Int J Surg Case Rep 53: 358-361, 2018.
10. Wang ZQ, Li JS, Lu GM, Zhang XH, Chen ZQ and Meng K: Correlation of CT enhancement, tumor angiogenesis and pathologic grading of pancreatic carcinoma. World J Gastroenterol 9: 2100-2104, 2003.
11. Horiguchi S, Kato H, Shiraha H, Tsutsumi K, Yamamoto N, Matsumoto K, Tomoda T, Uchida D, Akimoto Y, Mizukawa S, *et al*: Dynamic computed tomography is useful for prediction of pathological grade in pancreatic neuroendocrine neoplasm. J Gastroenterol Hepatol 32: 925-931, 2017.
12. Wilson NM, Masoud AM, Barsoum HB, Refaat MM, Moustafa MI and Kamal TA: Correlation of power Doppler with microvessel density in assessing prostate needle biopsy. Clin Radiol 59: 946-950, 2004.
13. Wei SC, Xu L, Li WH, Li Y, Guo SF, Sun XR and Li WW: Risk stratification in GIST: Shape quantification with CT is a predictive factor. Eur Radiol 30: 1856-1865, 2020.
14. Yamamoto N, Kato H, Tomoda T, Matsumoto K, Sakakihara I, Noma Y, Horiguchi S, Harada R, Tsutsumi K, Hori K, *et al*: Contrast-enhanced harmonic endoscopic ultrasonography with time-intensity curve analysis for intraductal papillary mucinous neoplasms of the pancreas. Endoscopy 48: 26-34, 2016.
15. Zhuang H, Yang ZG, Chen HJ, Peng YL and Li L: Time-intensity curve parameters in colorectal tumours measured using double contrast-enhanced ultrasound: Correlations with tumour angiogenesis. Colorectal Dis 14: 181-187, 2012.
16. Basilio-de Oliveira RP and Pannai VLN: Prognostic angiogenic markers (endoglin, VEGF, CD31) and tumor cell proliferation (Ki67) for gastrointestinal stromal tumors. World J Gastroenterol 21: 6924-6930, 2015.
17. Imamura M, Yamamoto H, Nakamura N, Oda Y, Yao T, Kakeji Y, Baba H, Maehara Y and Tsuneyoshi M: Prognostic significance of angiogenesis in gastrointestinal stromal tumor. Mod Pathol 20: 529-537, 2007.
18. Plate KH, Breier G, Weich HA and Risau W: Vascular endothelial growth factor is a potential tumour angiogenesis factor in human gliomas in vivo. Nature 359: 845-848, 1992.